Supporting Information

Yordanov et al. 10.1073/pnas.1405621111

SI Materials and Methods

Activation Tagging, Field Trial, and Screening for Bud Phenology. The activation tagging population was generated in the 717-1B4 (*Populus tremula* × *Populus alba*) genotype as previously described (1) and referred to as WT-717. A field trial of 627 independent transformation events and untransformed WT-717 plants was established in western Oregon. Each event was represented by four ramets. Measuring the time of bud-break was performed by daily visits and scoring bud-break. Events that displayed changes in their bud phenology in all four ramets were clonally propagated, and the observed phenotype was validated in a controlled growth chamber experiment (see below).

Plant Material and Treatments. Tissues for expression analysis were collected from WT-717 and transgenic plants grown in the greenhouse under normal fertilization, irrigation, and pest control conditions. All tissues were collected at the same time of the day (11:00 AM), immediately frozen in liquid nitrogen, and kept at −80 °C until processed. Young sylleptic branches of control 717 plants were immersed in 1:2 Murashige Skoog solution supplemented with 6-Benzylaminopurine (BAP) (0.5 mg/L) after treatment with 2,4-Dichlorophenoxyacetic acid (2, 4-D) (1.0 mg/L)].

For analysis of Early Bud-Break 1 (*EBB1*) expression during dormancy, we collected buds from two individual aspen (*Populus tremuloides*) trees for each month of the dormancy period (September to June). Whole buds were immediately frozen in liquid nitrogen and stored at −80 °C until processed. Scales were removed before RNA extraction.

We used photoperiodic inductive treatments to elicit dormancy as previously described (2). Actively growing plants were subject to a short-day photoperiod (16 h dark/8 h light) at 100 $\mu mol \cdot m^{-2} \cdot s^{-1}$ of photosynthetic photon flux, ∼60% humidity, and 21 °C constant temperature until bud-set (∼6–9 wk). Plants were then transferred to 4 °C for 11 wk to meet their chilling requirement, and subsequently moved to a greenhouse under a long-day photoperiod (8 h dark/16 h light) and 21 °C. The date of bud-break was monitored and recorded daily.

Regeneration capacity of leaf explants from 1-mo-old in vitro plants from WT-717 and *EBB1-overexpression* (*EBB1-oe*) lines was tested as previously described (3) without antibiotics in the media. Shoots (>1 mm) per explant were counted after 1 mo on shoot induction media.

Plasmid Rescue, Positioning of the Tag, and Sequence Analyses. To position the activation tag in *EBB1* mutant, genomic DNA flanking the insertion site was recovered via plasmid rescue as previously described (1). The EcoRI-rescued plasmid was sequenced using primer pSK0015E1 (5′-ATGGATAAATAGCCTTGCTTCC-3′) (accession no. GU124151). Sequence homology searches and sequence analyses were performed using the *Populus trichocarpa* genome portal (www.phytozome.net/), the National Center for Biotechnology Information BLAST server (www.ncbi.nlm.nih.gov/BLAST/), and the University of Wisconsin Genetics Computer Group software package (4). Sequence alignments were carried out by CLUSTAL W (5). The phylogenetic tree was built using MEGA4 (6), neighbor-joining, and 1,000 bootstrap replications.

Analysis of Transcript Abundance. RNA was extracted as previously described (1) and DNase-treated using a DNA-free TM kit (Ambion, Life Technologies). cDNA was synthesized using SuperScriptII (Invitrogen, Life Technologies) and 1–5 μg of total RNA. Primers used in the various experiments were as follows: (*i*) verification of *EBB1* activation and cytokinin induction [190F2 (5′-GGAATACCGAGCCATACAC-3′) and 190R2 (5′-GAAAGTAAAAGGAGGGAGCAAG-3′)], (*ii*) *EBB1* transcript in buds of wild aspen growing trees [LP (5′-AAATTGCTGTTCTCTCGGTCAC-3′) and RP (5′-ATCGGATGGTTCTTGTGGAA-3′)], (*iii*) *EBB1* transcript in four independent plant lines with suppressed *EBB1* expression (*amiEBB1*) plants [qEBB1-F (5′-TAGCAATGCGTGGTCTCAAGGC-3′) and qEBB1-R (5′-TATGAGCAGGGTCAGCTGTTGC-3′), and (*iv*) validation of microarray results (Table S2). An equal amount of cDNA was used in each reaction. Ubiquitin-like (Ubq) transcript was used as a loading control as previously described (1). Gel images were acquired by the Gel Doc-It (UVP) documentation system and quantified using ImageJ (National Institutes of Health; available at http://rsb.info.nih.gov/ij/index.html). Quantitative real-time RT-PCR was performed using a StepOnePlus Real-Time PCR System (Applied Biosystems, Life Technologies) using Maxima SYBR Green qPCR master mix (Thermo Scientific Co.), 0.1 μM each primer, and 2 μL of cDNA (10× diluted for ubiquitin expression) in a 20-μL final volume. The default StepOnePlus cycling parameters were used. All samples were run in three biological replicates, and relative transcript abundance was calculated using ubiquitin as an internal standard (7, 8).

Generation of Binary Vector Constructs and Transformation. *EBB1* was amplified using the following primers: K190F1_XhoI (5′-CTCGAGATGGAAGAAGCGCTTA-3′) and K-190-R1_XbaI (5′-TCTAGACTAAAAGCTGGCAGCAAA-3′). The amplified fragment was ligated into pART7 vector (9) using XhoI/XbaI cohesive ends between *CaMV 35S* promoter and ocs' terminator, and sequenced in both directions (accession no. GU124150). The whole expression cassette was released from the pART7 vector using NotI restriction and ligated into the pART27 binary vector at the corresponding NotI site. The generation of an amiEBB1 construct was done essentially as previously described (10). The amiEBB1 was produced by replacing the micro-RNA (miRNA) in the MIR164b sequence with miRNA: TTAACGACCCCATGGCGTCCC and miRNA*: GGAACGCCATGGGCTCGTTAT sequences. These sequences specifically target EBB1 and have mismatches at three nucleotides. For convenient cloning, B1 and B2 recombination site sequences were included in the 5′ and 3′ ends, respectively. The whole amiEBB1 sequence was synthesized in the pUC19 SmaI site (www.biomatik.com/). The resulting construct was cloned first into pDONR221 and then into pK7WG2 (11) using Gateway BP and LR recombination reactions respectively (Invitrogen, Life Technologies). The construct was sequence-verified for putative mutations introduced by the PCR amplification and transformed into *Agrobacterium* strain C58 using the freeze/thaw method (12). Colonies growing on selection media were PCR-verified for the presence of the binary vector. *Agrobacterium*-mediated transformation was performed as previously described (3) into the same genetic background (e.g., clone 717) in which the *EBB1* mutation was identified. Transgenic plants carrying the construct were recovered and PCR-verified for the presence of the transgene using p2735CI190F (5′-CTCGAGATGGAAGAAGCGCTTA-3′) and p2735CI190R (5′-TCTAGACTAAAAGCTGGCAGCAAA-3′) for EBB1-oe and amiEBB1-2F (TGCTGACCCACAGATGGTTA) plants and amiEBB1-2R (CATGGCGTTCCGAACTAACT) for amiEBB1 plants.

Microscopy and in Situ RT-PCR Analysis. Buds and apices from WT-717 and transgenic plants were sampled at the same time, immediately fixed in FAA, and embedded using Shandon Excelsior and Histocentre 2 (Thermo Scientific Co.). Five-micrometer thick sections were stained with H&E. Images were captured using a Leitz Wetzlar fluorescent microscope (Leica Microsystems GmbH) with a SPOT Insight QC camera and advanced SPOT software (Diagnostic Instruments, Inc.). Measurements were made from images in ImageJ 1.38v software.

To measure cell division, apices were sampled (five independent lines, one plant per line), and all subtending leaf primordia were carefully removed until the shoot apical meristem was exposed, fixed in 1:3 acetic acid/ethanol, and stained with acid-carmine (13) to visualize the dividing nuclei. Approximately 2,000 cells were inspected, and the mitotic phase was recorded. For in situ RT-PCR, we followed a previously published procedure with minor modifications (14).

Microarray Hybridization and Data Analysis. Collection and analysis of data were compliant with minimum information about a microarray experiment standards (15). For each genotype, two independent biological replicates were obtained. RNA was isolated as previously described using the Qiagen RNeasy Plant Kit (1). Before labeling, RNA quality was assessed by an Agilent Bioanalyzer (Agilent Technologies) and total RNA was used to prepare biotinylated cRNA. The labeling, hybridization, and imaging procedures were performed according to Affymetrix protocols using the Affymetrix Poplar GeneChip at the Center for Genomics Research and Biocomputing, Oregon State University, or at the Integrated Genomics Facility at Kansas State University. Data were analyzed using TM4:MeV software (16, 17). Raw data were normalized using the robust multiarray average algorithm (18). All microarray data generated have been deposited in the GEO database (accession nos. GSE16495 and GSE55813). To identify genes with significant differential transcript abundance, the probe sets that passed filtering were subjected to ANOVA ($P < 0.01$), followed by the more stringent LIMMA procedure (19) with a false discovery rate of 0.01, resulting in 4,960 probe sets. To increase the stringency and accuracy further, the probe sets were additionally analyzed with the Pavlidis Template Matching (PTM) procedure (20, 21) using EBB1 affymetrix probe (PtpAffx.208288.1.S1_at) as a template (with correlation $R > [\pm 0.8]$ and significance $P < 0.05$), resulting in 1,031 differentially expressed probe sets (corresponding to 971 genes). Fifteen differentially abundant gene transcripts were validated using semiquantitative RT-PCR and the same RNA used in the microarray experiments. Gene ontology (GO) analyses for significant enrichments of various categories were performed using agriGO (22), and the corresponding Arabidopsis Genome Initiative (The Arabidopsis Information Resource 9) genome loci. For identification of the EBB1 potential target genes, the −3,000 bp upstream promoter regions of the PTM positively correlated genes were used. Each promoter was searched with MeV software for the presence of a GCC-box: GCCGCC or CGGCGG (23).

1. Busov VB, et al. (2003) Activation tagging of a dominant gibberellin catabolism gene (GA 2-oxidase) from poplar that regulates tree stature. *Plant Physiol* 132(3): 1283–1291.
2. Rohde A, et al. (2007) Gene expression during the induction, maintenance, and release of dormancy in apical buds of poplar. *J Exp Bot* 58(15-16):4047–4060.
3. Han KH, Meilan R, Ma C, Strauss SH (2000) An *Agrobacterium tumefaciens* transformation protocol effective on a variety of cottonwood hybrids (genus *Populus*). *Plant Cell Rep* 19(3):315–320.
4. Devereux J, Haeberli P, Smithies O (1984) A comprehensive set of sequence analysis programs for the VAX. *Nucleic Acids Res* 12(1 Pt 1):387–395.
5. Thompson JD, Higgins DG, Gibson TJ (1994) CLUSTAL W: Improving the sensitivity of progressive multiple sequence alignment through sequence weighting, position-specific gap penalties and weight matrix choice. *Nucleic Acids Res* 22(22):4673–4680.
6. Tamura K, Dudley J, Nei M, Kumar S (2007) MEGA4: Molecular evolutionary genetics analysis (MEGA) software version 4.0. *Mol Biol Evol* 24(8):1596–1599.
7. Livak KJ, Schmittgen TD (2001) Analysis of relative gene expression data using real-time quantitative PCR and the 2(-Delta Delta C(T)) Method. *Methods* 25(4):402–408.
8. Tsai CJ, Harding SA, Tschaplinski TJ, Lindroth RL, Yuan Y (2006) Genome-wide analysis of the structural genes regulating defense phenylpropanoid metabolism in Populus. *New Phytol* 172(1):47–62.
9. Gleave AP (1992) A versatile binary vector system with a T-DNA organisational structure conducive to efficient integration of cloned DNA into the plant genome. *Plant Mol Biol* 20(6):1203–1207.
10. Du J, Mansfield SD, Groover AT (2009) The Populus homeobox gene ARBORKNOX2 regulates cell differentiation during secondary growth. *Plant J* 60(6):1000–1014.
11. Karimi M, Inzé D, Depicker A (2002) GATEWAY vectors for Agrobacterium-mediated plant transformation. *Trends Plant Sci* 7(5):193–195.
12. Holsters M, et al. (1978) Transfection and transformation of Agrobacterium tumefaciens. *Mol Gen Genet* 163(2):181–187.
13. Snow R (1963) Alcoholic hydrochloric acid-carmine as a stain for chromosomes in squash preparations. *Stain Technol* 38:9–13.
14. Johansen B (1997) In situ PCR on plant material with sub-cellular resolution. *Ann Bot* 80(5):697–700.
15. Brazma A, et al. (2001) Minimum information about a microarray experiment (MIAME)-toward standards for microarray data. *Nat Genet* 29(4):365–371.
16. Saeed AI, et al. (2003) TM4: A free, open-source system for microarray data management and analysis. *Biotechniques* 34(2):374–378.
17. Chu VT, Gottardo R, Raftery AE, Bumgarner RE, Yeung KY (2008) MeV+R: Using MeV as a graphical user interface for Bioconductor applications in microarray analysis. *Genome Biol* 9(7):R118.
18. Bolstad BM, Irizarry RA, Astrand M, Speed TP (2003) A comparison of normalization methods for high density oligonucleotide array data based on variance and bias. *Bioinformatics* 19(2):185–193.
19. Smyth GK (2005) Limma: Linear models for microarray data. *Bioinformatics and Computational Biology Solutions Using R and Bioconductor, R* (Springer, New York), pp 397–420.
20. Pavlidis P, Noble WS (2001) Analysis of strain and regional variation in gene expression in mouse brain. *Genome Biol* 2(10):H0042.
21. Yordanov YS, Regan S, Busov V (2010) Members of the LATERAL ORGAN BOUNDARIES DOMAIN transcription factor family are involved in the regulation of secondary growth in Populus. *Plant Cell* 22(11):3662–3677.
22. Du Z, Zhou X, Ling Y, Zhang Z, Su Z (2010) agriGO: A GO analysis toolkit for the agricultural community. *Nucleic Acids Res* 38(Web Server issue):W64–W70.
23. Eklund DM, et al. (2011) Expression of Arabidopsis SHORT INTERNODES/STYLISH family genes in auxin biosynthesis zones of aerial organs is dependent on a GCC box-like regulatory element. *Plant Physiol* 157(4):2069–2080.

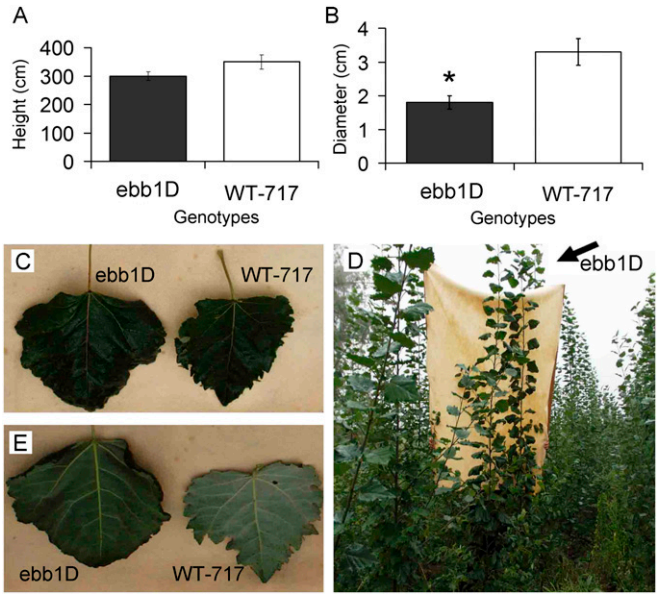

Fig. S1. Growth and morphology of *early bud-break 1 dominant* (*ebb1D*) mutant in the field. Height (*A*) and diameter (*B*) of 3-y-old field-grown *EARLY BUD-BREAK 1* (*EBB1*) and WT-717 (*Populus tremula* × *Populus alba* Institut National de la Recherche Agronomique 717-IB4) plants. Bars represent mean and SE from four ramets. *$P < 0.05$, Student *t* test. Adaxial (*C*) and abaxial (*D*) sides of leaves from field-grown *ebb1D* and WT-717 plants. (*E*) Whole-plant view of *ebb1D* trees in the field (in front of a light-colored cloth screen).

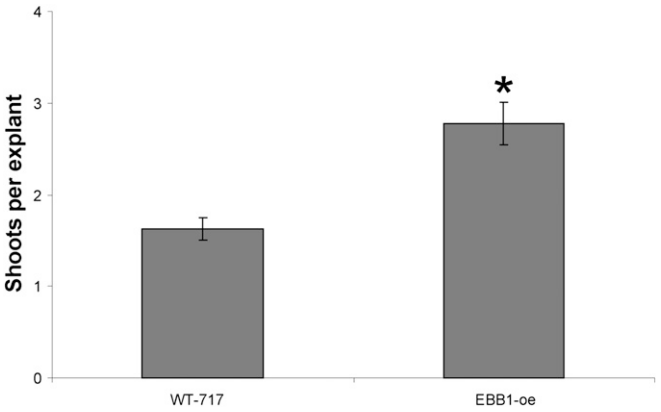

Fig. S2. Shoot regeneration from leaf segments. Leaf segments from WT-717 and *EBB1* overexpression (*EBB1-oe*) transgenic events ($n = 3$) were cultivated on callus induction media (1) for 3 wk and transferred on shoot induction media for 4 wk, and the number of regenerated shoots was recorded. Bars represent mean and SE from five biological replicates with 20 explants each. *$P < 0.05$, Student *t* test.

1. Han KH, Meilan R, Ma C, Strauss SH (2000) An *Agrobacterium tumefaciens* transformation protocol effective on a variety of cottonwood hybrids (genus *Populus*). *Plant Cell Rep* 19(3): 315–320

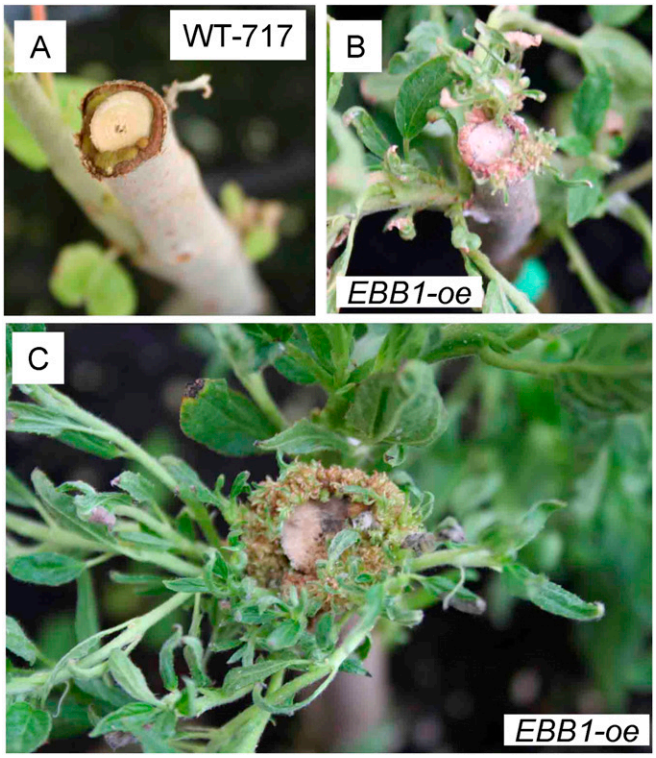

Fig. S3. Spontaneous shoot regeneration from cambium-derived callus in *EBB1-oe* transgenics. (*A*) WT-717 plants. (*B* and *C*) *EBB1-oe* transgenics. Stems were cut approximately a foot from the soil, and photographs taken 3 wk after cutting. Similar responses were seen in approximately one-half of the *EBB1-oe* transgenic events.

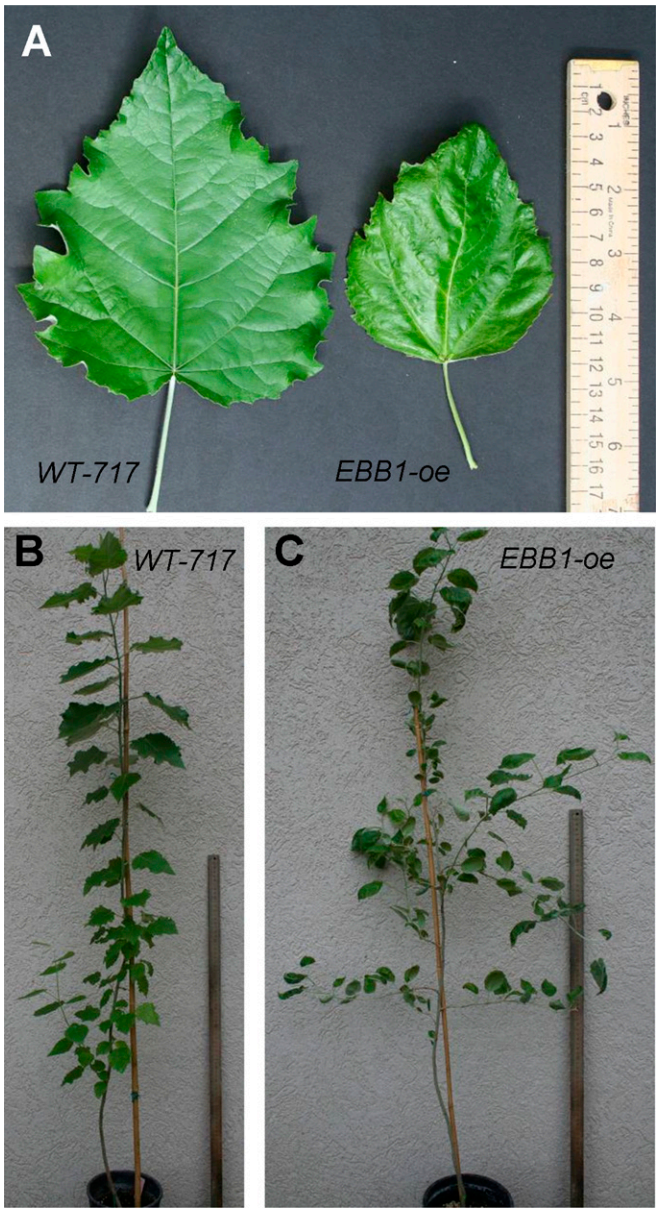

Fig. S4. Overexpression of *EBB1* causes a range of phenotypic changes. (*A*) Leaf size and form changes in *EBB1-oe* transgenics. Branching and size of WT-717 (*B*) and *EBB1-oe* (*C*) plants grown in a greenhouse for 4 mo.

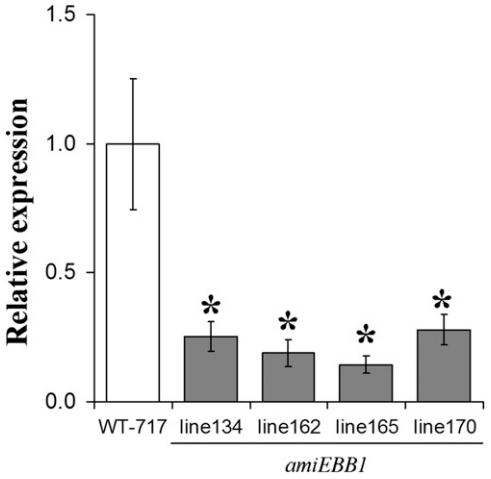

Fig. S5. Suppression of *EBB1* in four independent *amiEBB1* transgenic lines. Bars show 1 SE over genotypes' means ($n = 3$). Significance of differences was tested by the Student t test (*$P < 0.05$).

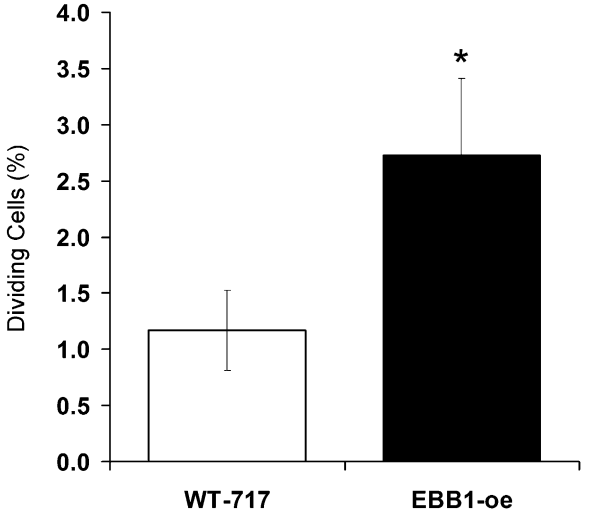

Fig. S6. Increased cell division rate in the apex of *EBB-oe* transgenics. Cells in metaphase, anaphase, and telophase were counted as dividing. The graph presents mean and SE of 10–12 acid-carmine–stained apices and ~2,000 cells. *$P < 0.05$, Student t test.

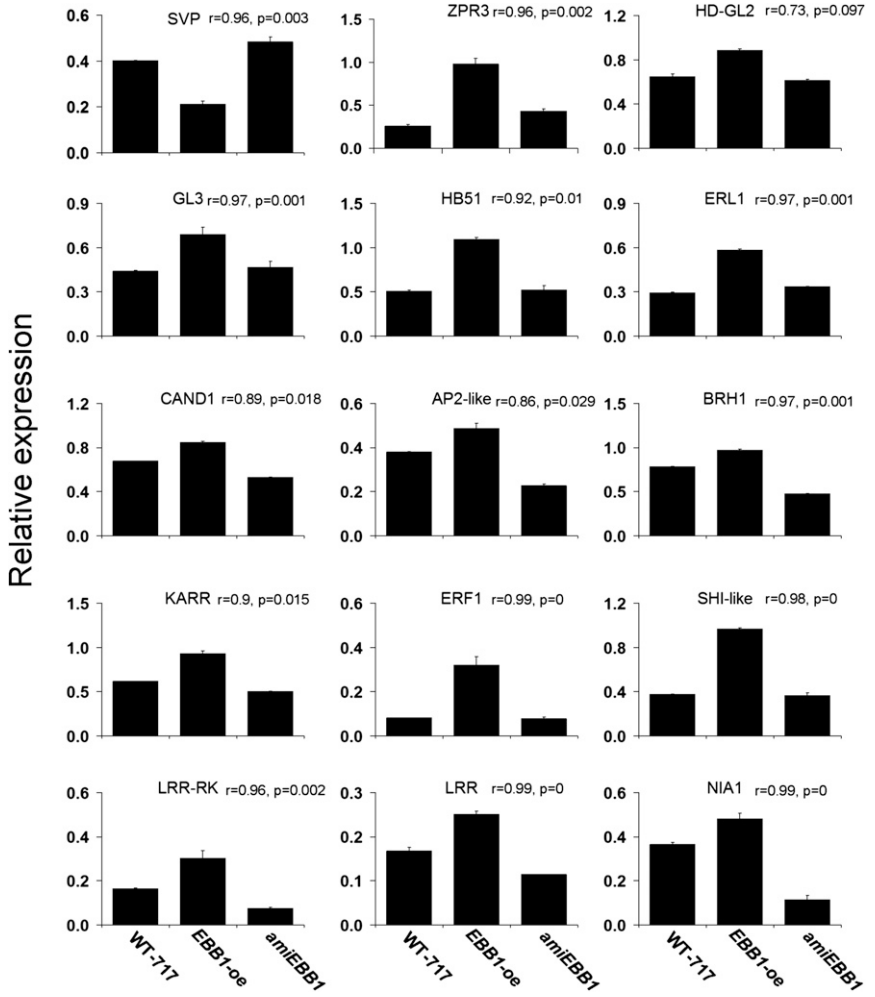

Fig. S7. Validation of microarray results. Bars represent mean and SE over two independent biological replications. Abbreviations used in the figure correspond to the names and gene models specified in Table S2. All expression estimates were normalized using ubiquitin gene expression as described above. In each graph, r and p indicate the correlation coefficient and the associated probability, respectively, between RT-PCR and microarray analyses.

Table S1. ***EARLY BUD-BREAK 1* (*EBB1*) gene subfamily in *Populus trichocarpa* genome**

Name	Model	Chromosome
Poptr51	Potri.017G053700	17
Poptr52	Potri.001G313500	1
Poptr60	Potri.010G046600	10
Poptr61	Potri.008G186300	8
Poptr63	Potri.008G215600	8
Poptr64	Potri.003G161000	3
Poptr65	Potri.001G069300	1
Poptr66	Potri.003G077700	3
Poptr67	Potri.001G157100	1

Poptr and Potri, *Populus trichocarpa* genome.

Table S2. Primers used for validation of microarray results

Gene model v3.0	Gene name	Forward primer	Reverse primer
Potri.007G010800	SVP	TGAGAGACTCAAACAGCAAGTGG	ACTGCCCTTCCTCGTAACCAAC
Potri.006G132400	AP2	ATGGTGGCGGAGCAAATCCACT	TGCTGGGGTTGGTAAATGGAGGAA
Potri.005G223200	ERF1	GATGTGAAGATGGGTGTTCGCCTGT	TTCCAGGTAGTCAGCTCCCAAATCCTC
Potri.012G130400	ERL1	TCTTGCAAGTTGCTACTCTGTCC	GGCCTGCATTAAACCAATCACTTC
Potri.014G083900	GL3	AGGGTTGCCAGGAAGAGCATTAG	TCTGAATTGATGCGCTCTTTGCG
Potri.002G230200	HD-GL2	GATGAGAACACCCGTAATGAGTGG	GTGTGCCATTTCTTGGACAACCC
Potri.006G083200	ZPR3	GCACAGCTTCTCAACCAGGAG	AGTTGGGCTTGGAGAGTTTCTGC
Potri.006G117700	HB51	TCCAGGCATGGACATGAAGCAC	ACTGGTCACTTGTCAATCGCTTC
Potri.003G003500	CAND1	GGACCGCAACTACGCAAGGATAAG	TTGCATCCCATGAGCAGCAGAG
Potri.011G150800	BRH1	CGATTCCAGTCCCAGTTTCCGTTC	AGCTGCTGAATGCCATCACTGG
Potri.003G196100	SHI	CAGGATGCAAGCTTCAAACAGTCC	CATAGGCAACCTCAGCTTCATCAC
Potri.001G385400	LRR-RK	TGTCTCTTCTGGCAAACCGTCTC	AGGGACTTCAGAGTCGCAAAGC
Potri.014G024300	LRR	GGTGGAGCTGCTGAACTTTACTGG	TTTCCAGCTCACAGACCACCTC
Potri.002G088600	NIA1	ACTGCCCTCGCATGTTGATACAG	CTCTGTCTTGTACCACCAGGCTTC
Potri.015G116800	KARR	GCGTCTGATGCTTCTGATTGCG	ACCTGTGTGATCTTCGACTTCGG

SVP, SHORT VEGETATIVE PHASE; AP2, APETALA2; ERF1, ETHYLENE RESPONSE FACTOR 1; ERL1, ERECTA-LIKE 1; GL3, GLABROUS 3; HD-G2, HOMEODOMAIN GLABROUS 2; ZPR3, LITTLE ZIPPER 3; HB51, HOMEOBOX 51; CAND1, CANDIDATE G-PROTEIN COUPLED RECEPTOR 1; BRH1, BRASSINOSTEROID-RESPONSIVE RING-H2-1; SHI, SHORT INTERNODES; LRR-RK, LEUCINE-RICH REPEAT RECEPTOR KINASE; LRR, LEUCINE-RICH REPEAT; NIA1, NITRATE REDUCTASE 1; KARR, KARRIKIN responsive.

Other Supporting Information Files

Dataset S1 (XLS)
Dataset S2 (XLS)
Dataset S3 (XLS)
Dataset S4 (XLS)
Dataset S5 (XLS)
Dataset S6 (XLS)